

Photosynthetic response of wheat to stress induced by *Puccinia recondita* and post-infection drought

O. BETHENOD^{*,***}, L. HUBER^{*}, and H. SLIMI^{**}

Institut National de la Recherche Agronomique, Unité mixte de Recherche Environnement et Grandes Cultures, 78850 Thiverval-Grignon, France^{*}

International Centre for Advanced Mediterranean Agronomic Studies, Bari, 70010 Italy^{**}

Abstract

To quantify photosynthetic response of wheat to the combination of a fungal brown rust infection and a post-infection drought, four treatments were compared: no stress (control), fungal stress (FS), water stress (WS), and twofold stress (WS×FS). Predawn leaf water potential (Ψ_{wp}) was similar in FS and WS treatments over a 3-week period. In the WS treatment, net photosynthetic rate (P_N) and stomata CO_2 conductance (g_s) diminished concomitantly with a constant intercellular CO_2 concentration (C_i) close to 200 $\mu\text{mol mol}^{-1}$. In the FS treatment, a reduction of P_N occurred with an increase in respiration rate (doubling of the CO_2 compensation concentration) and in C_i but with no water loss modification. Healthy leaves of infected plants (FS) showed a reduction of P_N as well, with constant g_s and increased C_i . In the twofold stress treatment (WS×FS), leaves showed reduced P_N in relation to the lower Ψ_{wp} . Deleterious effects of both drought and fungal infection on the final area of leaves and dry matter were additive.

Additional key words: biotic stress; brown rust; intercellular CO_2 concentration; leaf gas exchange; plant growth; respiration rate; stomata conductance; stress interaction; *Triticum aestivum* L.; water stress.

Introduction

Flag leaves of wheat plants infected by *Puccinia recondita* f. sp. *tritici* showed a decrease in the net photosynthetic rate (P_N) per leaf area unit and per chlorophyll (Chl) unit as well as a decrease in transpiration rate (McGrath and Pennypacker 1990). Wheat cultivars susceptible to brown rust had reduced P_N and increased Chl content, whereas no modification was observed in resistant cultivars (Statler 1988). Changes in P_N also exist in healthy leaves of infected plants (Murray and Walters 1992).

The effects of fungal stress on leaf transpiration rate (E) are well documented (Ayres 1981). The decrease in E results from the stomata closure following infection by pathogens, the intoxicating action upon host cells, the reduction of air spaces by fungal hyphae, and the possible obstruction of vessels and stomata (Duniway and Durbin 1971). Working on wheat flag leaves, McGrath and Pennypacker (1990) have shown that brown rust induces an E reduction before sporulation. After sporulation, water losses from infected tissue increased primarily through epidermal rupture and through stomata that re-

mained open even under dark or dry conditions. The acceleration of water loss by infected tissues can frequently be attributed to epidermal ruptures (Spotts and Ferree 1979, Tissera and Ayres 1986), to inhibition of stomatal closure (Turner and Graniti 1969), to direct loss from the parasite tissues, or increase in host tissue permeability induced by the secretion of enzymes or fungal toxins (Arntzen *et al.* 1973).

At plant level, the photosynthesis reduction in wheat plants infected by stem rust has been explained by a decrease in leaf area and by a reduction in CO_2 assimilation efficiency (Berghaus and Reisener 1985), by a decrease in Chl content, by an inhibition in photosynthetic phosphorylation, by modifications in the Hill reaction and CO_2 assimilation (Spotts and Ferree 1979) and in translocation of photosynthates (Okwulehie 2000). In various pathogenic systems studied under field conditions, reductions of P_N and E at plant level were caused by early defoliation and leaf drying linked to fungal development and resulted in cell damage and death (Shtienberg 1992). In this field study it was shown that the decrease in P_N

Received 18 June 2001, accepted 20 August 2001.

***Corresponding author; fax: +33 (0)1 30 81 55 63; e-mail: bethenod@grignon.inra.fr

Acknowledgements: We thank H. Autret, R. Goujet, and D. Renard for excellent and skilful technical assistance in gas exchange measurements, statistical analysis, and plant growth chamber monitoring, respectively. For using facilities of Plant Pathology and Epidemiology Laboratory, INRA, the help of C. de Vallavieille-Pope, I. Sache, and L. Geagea is gratefully acknowledged.

or E was not proportional to the corresponding reduction in healthy leaf area due to disease. However, the pattern of plant response to disease was related to the types of trophic relationship.

For biotrophic fungi such as rusts, the equilibrium modification between water absorbed by roots and the transpiration demand depends on the infected leaf area and the type of infection site. As disease progressed, barley leaves infected by *Puccinia hordei* lose their ability to keep a favourable water status (Berryman *et al.* 1991). A rapid decrease in soil water content caused a slight reduction in the water potential of sugar beet leaves infected by *Erysiphe poligoni* when only the first leaf showed disease symptoms. However, a noticeable reduction can occur when symptoms appear on the first to the seventh or eighth leaves (Gordon and Duniway 1982).

On faba bean leaves infected by rust (*Uromyces viciae faba*), the water potential of diseased leaves was lower than in healthy leaves (Tissera and Ayres 1986). Following epidermal rupture due to rust lesions, E of the groundsel plant increased and led to a water potential reduction (Paul and Ayres 1984). Under such unfavourable water regime there was a significant limitation in water use efficiency (Balasubramanian and Gaunt 1990).

Materials and methods

Plants: Wheat (*Triticum aestivum* L. cv. Michigan Amber) seedlings sensitive to brown rust were grown in a climatic chamber. Healthy seeds were sown in 11×11 cm plastic pots (4 seeds per pot). Environment in the growth chamber was favourable to both plant growth and disease development. The temperature was 17±1 °C during the 16-h light period and 15±1 °C during the 8-h dark period. At 0.8 m from the light sources, the spatial mean of radiation was 416±40 $\mu\text{mol m}^{-2} \text{s}^{-1}$. Transpiration and irrigation were controlled by weighing pots using load cells (*Scaime, AG 30*, Annemasse, France) connected to a data logger (*Campbell, CR7*, Shepshed, UK). This method made it possible to estimate the amounts of irrigation on a daily basis.

Fungal pathogens and inoculation procedure: Plants bearing sporulating lesions were produced under the conditions described above (see also Geagea *et al.* 1999). Five leaf seedlings of the susceptible cultivar were uniformly inoculated in a settling tower with (uredo) spores of brown rust (*Puccinia recondita* f. sp. *tritici*) using a density of 345±30 spores per cm^2 (in one type of experiment 3 leaf seedlings were used). After 24 h in controlled conditions conducive to infection, seedlings were transferred into the growth room for incubation. The experiments lasted from the 5th to the 20th day after inoculation.

Experimental protocol: Four treatments were consid-

It is important to know whether the effects of interacting water stress and fungal constraint are additive. For example, a reduction in P_N and leaf area was noticed on leaves of groundsel plants infected by rust and temporarily water-stressed under laboratory conditions (Paul and Ayres 1984). This issue has been analysed in the field on wheat to quantify the effects of water stress along with leaf blotch and brown rust diseases; this field work was done under temperate climate (Cowan and Van der Wal 1975) as well as under semi-arid conditions (Shtienberg 1990).

Based on leaf gas exchange techniques and plant growth characterisation, our objective was to quantify the response of wheat leaves to the combination of brown rust infection and post-infection drought in comparison to each single stress. To investigate to what extent leaf P_N and growth reductions of infected wheat plants could be explained by the water stress caused by either brown rust or post-infection drought, response curves of P_N to irradiance and CO_2 concentration were used. To interpret experiments on irradiance response curves obtained in different conditions of infection and post-infection drought, a simple analytical model including parameters dependent on predawn leaf water potential was tested.

ered: control, water stress (WS), fungal stress (FS), and double stress (WS×FS). The water-stressed treatment started the second day after the inoculation date. Water stress was obtained by applying only 50 % of daily transpiration measured on control plants; FS plants were irrigated according to the water loss of the previous day. In these four treatments, measurements were taken 4 d after inoculation (before sporulation), 11 d after inoculation (just after sporulation), and 18 d after inoculation. Physiological measurements determined plant growth, and water potential and gas exchange of leaves. By measuring the number of lesions per square cm, the disease could be assessed from the 5th d (just before measurements of leaf gas exchange) to the 22nd d after inoculation.

Plant growth and leaf water potential measurements: Dry matter was obtained by weighing individual plants dried at 80 °C for 72 h. Using an optical leaf area meter (*Li-Cor*, Lincoln, NE, USA), leaf area was measured on the 5th inoculated leaf, the 7th leaf (appearing before sporulation on the 5th leaf), and the 8th leaf (appearing after lesion appearance on the 5th leaf). During the experiment, the predawn leaf water potential (Ψ_{wp}) of 6 last fully developed leaves from 6 different pots was measured, 2 h before light start-up, using a Scholander type pressure chamber (*PMS Instruments*, Corvallis, OR, USA).

P_N and g_s in relation to disease and/or water stress: CO_2 and H_2O exchange were measured with a Parkinson leaf chamber connected to a CO_2 analyser (ADC, type LCA3, Hoddesdon, UK). This transient open gas exchange system allowed simultaneous estimate of P_N and g_s . It consists of a mass flow controller, a leaf chamber (where air temperature, humidity, and radiation are measured), an infrared gas analyser, and a data logger. The incoming air was furnished by a compressed air cylinder, the CO_2 concentration of which was $370 \mu\text{mol mol}^{-1}$. The individual P_N and g_s measurements took less than 1.5 min. P_N measurements started on the fourth day after inoculation. They were made each day 4 to 5 h after start of light period on leaves that were well exposed to radiation (10 leaves in 10 different pots for each of the four treatments). The range of incident photosynthetic photon flux (PPFD) density was $550\text{--}650 \mu\text{mol m}^{-2} \text{s}^{-1}$ inside the leaf chamber.

On leaves with lesions, $g_{s\text{H}_2\text{O}}$ values quantified water transfer rate through stomata and epidermal lesions. To calculate $g_{s\text{CO}_2}$, it was assumed that the diffusion ratio (1.6) between water and CO_2 was identical for both pathways. To calculate C_i , it was assumed that there was no obstacle to CO_2 diffusion in the intercellular spaces. Using this assumption, conductance measurements could be compared between the 4 treatments.

P_N response curves under controlled irradiance and CO_2 concentration: At a given CO_2 concentration, the relationship between P_N and incident radiation provides one way to characterise the plant responses to fungae and/or water stress (Fig. 1A). The corresponding curves use a non-rectangular hyperbola with 4 parameters: maximal radiation use efficiency (MRUE), dark respiration rate (R_D), convexity index (m), and maximal net photosynthetic rate ($P_{N\text{max}}$). The appendix describes how changes in the four parameters were modelled against plant water status expressed by predawn leaf water potential (Ψ_{wp}). In Fig. 1A, points H and S represent $P_{N\text{max}}$ values corresponding to control and stressed plants, respectively.

Changes in $P_{N\text{max}}$ values result from stress effects on stomata, CO_2 fixation, and respiration. To separate these 3 types of action, a response curve of P_N versus C_i was

Results

Growth: Both types of stress altered the dry matter dynamics. In the chosen growing conditions, a similar growth reduction was observed for WS and FS applied independently. The combination of both stresses reduced the plant dry matter by 22 %, which corresponds to the sum of reductions caused by WS alone (13 % reduction) and infection alone (8 % reduction). In the FS treatment, the leaf area reduction was similar for the three types of leaves (5th, 7th, or uninfected top leaves appearing on

obtained by varying the air CO_2 concentration (C_a) under saturating irradiance (Fig. 1B). Beside the general situation of change conducive to the reduction in $P_{N\text{max}}$ under non-limiting PPFD (from H to S in Fig. 1B), there are three more specific situations: (1) from H to Sg, a decrease in $g_{s\text{CO}_2}$ with no modification of the response curve $P_{N\text{max}}(C_i)$, (2) from H to Sm, a decrease in $P_{N\text{max}}$ with no modification of g_s , (3) an increase in respiration (photorespiration and R_D) rates with enhancement of the CO_2 compensation concentration Γ (from Γ_H to Γ_S). In all three situations, a decrease in $P_{N\text{max}}$ corresponds to either decreasing C_i due to stomata closure, or increasing C_i owing to non-stomatal effects, or enhanced R_D .

Measurements of P_N and g_s were made using a portable LI-6400 photosynthesis system (Li-Cor, Lincoln, NE, USA). This instrument allows generate reproducible conditions of irradiation, temperature, relative humidity, and CO_2 concentration. Estimated variables are P_N , $g_{s\text{CO}_2}$, and C_i (equal to $C_a - P_N/g_s$, corrected according to Caemmerer and Farquhar 1981). Response curves for P_N versus PPFD were established for 7 irradiances (0, 60, 120, 200, 500, 1 200, and 1 500 $\mu\text{mol m}^{-2} \text{s}^{-1}$) under an air CO_2 concentration of $350 \mu\text{mol mol}^{-1}$. Response curves for P_N versus C_i were obtained for 7 values of C_a (350, 300, 200, 150, 100, 50, 0 $\mu\text{mol mol}^{-1}$) under saturating irradiance ($1 500 \mu\text{mol m}^{-2} \text{s}^{-1}$). Each response curve to irradiance and CO_2 concentration was based on measurements made during 90 min per leaf.

Statistical analysis: The irradiance response curves of leaf photosynthesis were analysed using NLIN procedure of the Statistical Analysis System (SAS 1988). The appendix describes individual steps of this analysis. Except for photosynthesis response curves, all values shown are means of replicates (1 replicate = 1 leaf taken from one pot; number of replicates: 6 for Ψ_{wp} , 10 for photosynthesis and stomatal conductance ADC measurements, 12 for measurements of disease severity, leaf area, and plant growth). In most cases, variability estimates are given by the confidence interval for $p = 0.05$. The comparison of means was made using the Student's *t*-test between two treatments and the multiple range Duncan's test between 4 treatments using the ANOVA procedure of the Statistical Analysis System (SAS 1988).

inoculated leaves after the beginning of sporulation) (Table 1). In comparison to control plants, leaf area reduction was between 14 and 17 %. In the WS treatment, leaf area reductions were 19, 35, and 51 % for the 5th, 7th, and uninfected top leaf, respectively. In the WS×FS treatment, the leaf area reduction was 37 and 47 % on the 5th and 7th leaves, respectively. These reductions corresponded roughly to the sum of leaf area reductions obtained on plants submitted to the two types of stress ap-

Table 1. Leaf area [cm^2] for the four treatments: control, fungal stress (FS), water-stress (WS), and double stress (WS×FS) for three leaves categories: 5th, 7th, and non-inoculated top leaf. Means \pm SE.

	Control	FS	WS	FS×WS
5 th leaf (<i>n</i> = 22)	15.94 \pm 2.79	13.73 \pm 2.21	12.93 \pm 2.74	10.05 \pm 1.84
7 th leaf (<i>n</i> = 14)	17.40 \pm 3.19	14.66 \pm 2.02	11.38 \pm 1.91	9.29 \pm 1.13
top leaf (<i>n</i> = 14)	12.93 \pm 2.44	10.79 \pm 1.74	6.33 \pm 0.76	8.50 \pm 0.83

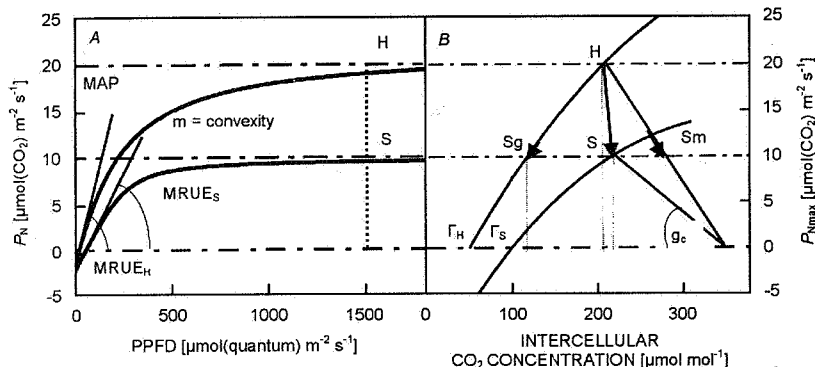


Fig. 1. Conceptual framework for examining (A) leaf net photosynthetic rate (P_N) responses for healthy (H) or stressed (S) plants to photosynthetic photon flux density (PPFD) under an air CO_2 concentration of $350 \mu\text{mol mol}^{-1}$ with corresponding changes in maximal net photosynthetic rate ($P_{N\text{max}}$), maximal radiation use efficiency (MRUE), and dark respiration rate (R_D), or (B) response of $P_{N\text{max}}$ to intercellular CO_2 concentration (C_i) under a given PPFD ($1500 \mu\text{mol m}^{-2} \text{s}^{-1}$). Both situations, H and S, are shown with corresponding changes in the CO_2 compensation concentration for P_N (Γ) and in epidermal CO_2 conductance (g_s) between air CO_2 concentration (C_a) and C_i .

plied independently. In contrast, on young uninfected leaves, the leaf area reduction in the WS×FS treatment was 34 %, which is the average of the FS (17 % reduc-

tion) and WS (51 % reduction) treatments.

Disease-water relationships: On both FS and WS×FS treatments, lesions appeared on the 8th day after inoculation (Fig. 2A). The number of lesions increased in relation to the number of infection cycles on inoculated leaves. In the WS×FS treatment, the lesion number increased gradually until the 19th d, and reached an asymptotic value slightly greater than 60 lesions per cm^2 . This threshold was partially due to the method of measurement, because the lesions tended to coalesce. The lesion number in the WS×FS treatment was always at least twice that of the FS treatment. The water status of control plants did not change significantly from day 12 to day 19 (Fig. 2B). In contrast, on the 12th d after inoculation, inoculated watered plants showed a significant change in the water status in comparison to control plants. The leaf water potentials in the WS and FS treatments were similar. In both treatments, water stress occurrence was indicated by pre-dawn leaf water potential below -0.3 MPa (Hsiao 1973). Under the chosen growing conditions, fungal development and the increase in water stress were concomitant in the WS×FS treatment. Owing to the added effects of both FS and WS, Ψ_{wp} was significantly lower than in the two single stress treatments.

When uredia appeared (9 d after inoculation), rust-infected leaves showed a strong reduction in pre-dawn leaf water potential: on diseased plants, Ψ_{wp} were -0.37 (FS) and -0.50 MPa (WS×FS), significantly lower than -0.25

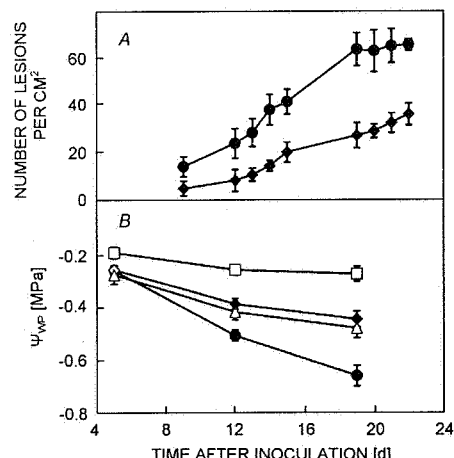


Fig. 2. (A) Time change in mean number of brown rust lesions per unit [cm^2] of inoculated leaf area in inoculated stressed (●) and irrigated (○) plants. Each point is the mean of 16 replicates; vertical bars represent the standard error. (B) Time change in predawn leaf water potential (Ψ_{wp}) for young healthy wheat plants (□), plants subjected to rust infection (◊) or water stress (Δ), and both infection and water stress (○). Each point is the mean of six replicates \pm one standard error. Open symbols correspond to measurements on days before sporulation; closed symbols correspond to measurements on days after the start of sporulation.

MPa (control) and -0.41 MPa (WS) in healthy plants. At the end of the experiment (19–22 d after inoculation), WS and FS plants showed a similar Ψ_{wp} . Nevertheless, Ψ_{wp} of the FS treatment was significantly higher than that of the WS treatment (-0.44 MPa and -0.48 MPa, respectively). The lowest Ψ_{wp} was obtained in the WS \times FS treatment (-0.63 MPa) exhibiting the highest lesion area density. Due to similar number of lesions on day 12 in the WS \times FS treatment and day 19 in the FS treatment, the Ψ_{wp} observed in the WS \times FS treatment was significantly lower.

From day 5 to day 19 after inoculation, *i.e.*, before and after sporulation, Ψ_{wp} was always slightly lower in the treatment with five inoculated leaves (Table 2).

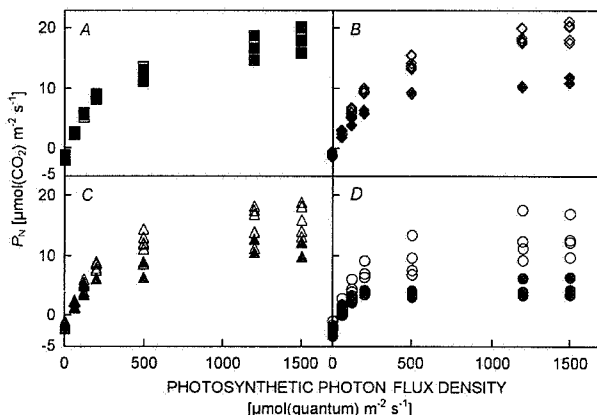


Fig. 3. Relationships between net photosynthetic rate (P_N) and photosynthetic photon flux density (PPFD) for (A) healthy wheat leaves (\square \blacksquare), (B) infected leaves (FS, \diamond \blacklozenge), (C) water-stressed leaves (WS, Δ \blacktriangle), and (D) double stressed leaves (WS \times FS, \circ \bullet). Open symbols correspond to measurements on days before sporulation; closed symbols correspond to measurements on days after sporulation start.

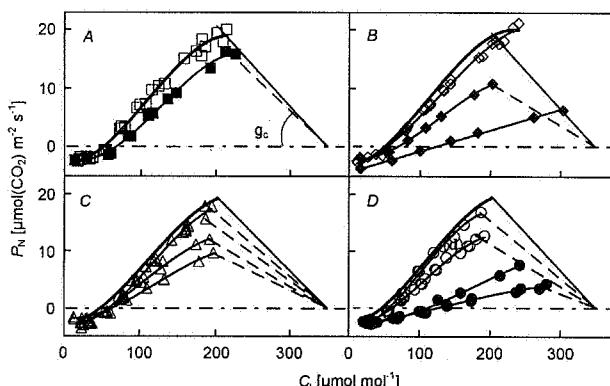


Fig. 4. Relationships between net photosynthetic rate (P_N) and intercellular CO_2 concentration (C_i) on the 5th leaf of wheat plants for the four treatments: control (A), fungal stress (B), water stress (C), and fungal \times water stress (D). The same symbols as in Fig. 3. The response curves are fitted to a third-order polynomial equation. The epidermal conductance for CO_2 (g_s) is shown as the line linking C_a and the corresponding point (P_N , C_i). On each of the 4 figures, thick lines represent response curves of control plants.

Leaf gas exchange: The control treatment (Fig. 3A) showed minor variations in the four parameters with the 5th leaf: dark respiration (R_D), maximal radiation use efficiency (MRUE), convexity (m), and $P_{N\max}$. In the FS treatment (Fig. 3B), two groups of plants could be distinguished according to sporulation occurrence. In non-sporulating plants, the irradiance response curves were similar, but in sporulating plants P_N was reduced. In the WS treatment (Fig. 3C) there was also a continuous reduction in both MRUE and $P_{N\max}$. In the WS \times FS treatment (Fig. 3D) two categories of response curve were observed: before sporulation, a continuous decrease in P_N , similar to the WS treatment, and after sporulation a very strong decrease in $P_{N\max}$.

Table 2. Time variation of predawn leaf water potential (PWLP, MPa) in relation to the infected leaf area (3 or 5 inoculated bottom leaves) by *Puccinia recondita*. Means \pm SE ($n = 6$). ** significantly different for $p = 1\%$, *** significant for $p = 0.1\%$.

Time after inoculation [d]	Ψ_{wp} (3 leaves)	Ψ_{wp} (5 leaves)
5	-0.20 ± 0.02	$-0.26 \pm 0.02^{**}$
12	-0.34 ± 0.02	$-0.39 \pm 0.02^{**}$
19	-0.38 ± 0.02	$-0.45 \pm 0.03^{***}$

The variations in P_N versus C_i under saturating irradiance ($1500 \mu\text{mol m}^{-2} \text{s}^{-1}$) allowed assess the magnitude of changes in $P_{N\max}$ (between $21.2 \mu\text{mol m}^{-2} \text{s}^{-1}$ and zero, Fig. 4). In control plants (Fig. 4A), P_N decreased slightly over time and Γ increased slightly. In the FS treatment, before sporulation, the same eco-physiological behaviour was observed for both P_N and Γ , with a concomitant decrease in $g_{s\text{CO}_2}$ (Fig. 4B). Upper curves showed a relatively constant C_i corresponding to C_a of $350 \mu\text{mol m}^{-2} \text{s}^{-1}$. When lesions were well developed (lower curve in Fig. 4C), Γ and g_s increased, the value of g_s becoming close to its initial value. These changes corresponded to a noticeable C_i increase. In the WS treatment (Fig. 4C), a progressive P_N reduction and stomata closure were concomitant with C_i , being approximately constant and unmodified in comparison to the control treatment. In the WS \times FS treatment (Fig. 4D) two types of response curve were observed before and after start of sporulation. Before sporulation the leaf P_N response was comparable to that of the WS treatment with concomitant P_N decrease and stomata closure. Under the chosen availability of soil water, there was no change in the calculated C_i , nor was the Γ value modified. After sporulation, a strong increase was noticed for both Γ and C_i (as in the FS treatment) with a correlative decrease in g_s .

In control plants (Fig. 5A), the ranges of P_N were comparable for newly formed leaves (after the sporulation date on infected plants) and 5th leaves (Figs. 5A and 4A). For these two categories of leaves, water stress determined a similar decrease in both P_N and g_s with no change in Γ (Figs. 5C and 4C). In contrast, for newly

formed FS leaves, there was a decrease in P_N with stable g_s and, therefore, an increase in C_i (Fig. 5B). For double stressed plants (WS×FS; Fig. 5D), stomata closure was observed (strong decrease in g_s) but both Γ and the initial slope of the P_N - C_i response curve remained unmodified.

To understand how changes in water status induced by rust infection could alter gas exchange, the P_N -PPFD curve was modelled analytically using the non-rectangular hyperbola whose parameters were estimated against changes in Ψ_{wp} for the four treatments (Table 3). MAP_{max} and $MRUE_{max}$ values were not significantly different from values estimated for control plants [$2.4 \pm 0.2 \mu\text{mol}(\text{CO}_2) \text{ m}^{-2} \text{ s}^{-1}$ compared to the confidence interval $22.0-24.4 \mu\text{mol}(\text{CO}_2) \text{ m}^{-2} \text{ s}^{-1}$ for MAP_{max} and confidence interval $0.067-0.075 \text{ mol}(\text{quantum}) \text{ mol}^{-1}(\text{CO}_2)$ compared to $0.073-0.09 \text{ mol}(\text{quantum}) \text{ mol}^{-1}(\text{CO}_2)$ for $MRUE_{max}$]. Minimal value of m , m_{min} , was fixed to 0.41 for control plants according to the confidence interval calculated as 0.36-0.46. A slope value of -2 for SL_p determines a zero value of P_{Nmax} for a Ψ_{wp} of -0.7 MPa. The SL_R value indicates that $MRUE$

decreased as Ψ_{wp} decreased whereas SL_m value indicates that the convexity increased with Ψ_{wp} .

The model expresses changes in non-rectangular hyperbola parameters according to the values estimated in Table 3 and assuming mean R_D of $-1.6 \mu\text{mol}(\text{CO}_2) \text{ m}^{-2} \text{ s}^{-1}$ (Fig. 6). Though the slope of the regression line was close to 1 (0.96 , $r^2 = 0.92$), note that WS×FS values are above the 1:1 line and WS values below it.

P_N measured in the growth chamber using *LCA3 ADC* diminished in response to the decrease in predawn leaf water potential derived using irradiance and Ψ_{wp} measurements and the hyperbolic function (Eq. 1 in Appendix). This independent data set shows that points belong to one single response relation (Fig. 7A). This hyperbolic response is close to the linear regression proposed for change in P_{Nmax} with a nil value of P_{Nmax} for Ψ_{wp} value of -0.7 MPa.

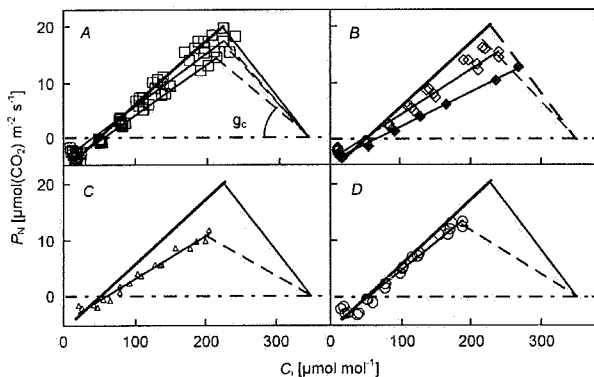


Fig. 5. Relationships between net photosynthetic rate (P_N) and intercellular CO_2 concentration (C_i) in healthy leaves appearing after inoculation at the top of infected plants. The same symbols as in Fig. 4.

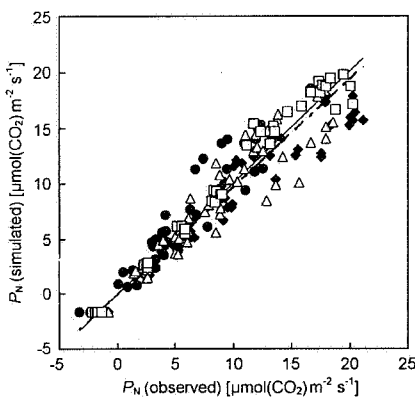


Fig. 6. Comparison of observed and modelled net photosynthetic rate, P_N , for the four treatments with observed values of the Fig. 3. The dotted line represents the linear regression between observed and modelled P_N ($AP_{modelled} = 0.96 AP_{observed}$, $r^2 = 0.92$). The 1:1 line is represented. Open symbols for healthy leaves (control: □; WS: Δ); closed symbols for inoculated leaves (FS: ◆; WS×FS: ●).

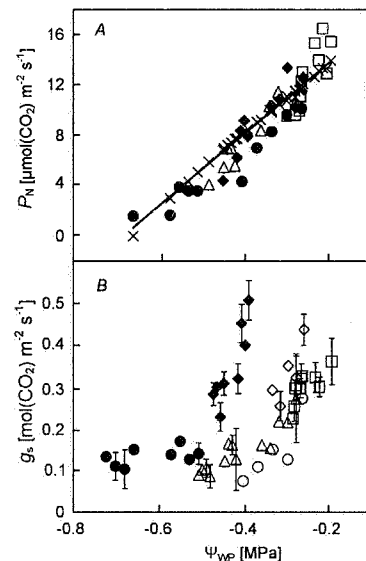


Fig. 7. (A) Relationship between net photosynthetic rate, P_N , and predawn leaf water potential (Ψ_{wp}), for the four treatments. Comparison of the P_N measurements made inside the growth chamber and the P_N modelled under a range of PPF between 550 and $650 \mu\text{mol m}^{-2} \text{ s}^{-1}$. The same symbols as in Fig. 6. Each point represents the mean value of 10 leaves from different plants. Line represents the linear regression between modelled values (X) and Ψ_{wp} . (B) Relationships of CO_2 diffusion conductance (g_s) and predawn leaf water potential (Ψ_{wp}) for the four treatments; the same symbols as in Fig. 3. Each point represents the mean value of 10 leaves from different plants. Vertical bars represent the standard error.

In control plants, g_{sCO_2} did not significantly change (Fig. 7B). From the day of inoculation to the beginning of sporulation (\diamond), g_s in FS was similar to g_s in control plants. At the beginning of sporulation (9 to 14 d after inoculation), g_s in FS plants was significantly higher (up to $0.5 \text{ mol m}^{-2} \text{ s}^{-1}$) than in control plants ($0.33 \text{ mol m}^{-2} \text{ s}^{-1}$), then (after day 14), g_s values in FS plants decreased to values similar to those of control plants. These results

indicate that brown rust sporulation induces a transient enhancement of water logging in the FS treatment. In WS plants, g_s continuously decreased. In WS×FS plants, g_s remained close to $0.15 \text{ mol m}^{-2} \text{ s}^{-1}$. Two different ranges of g_s were observed for irrigated plants (control and FS) and water-stressed plants (WS and WS×FS). In healthy

plants g_s decreased with decreasing predawn leaf water potential. In infected plants there was a lot of scattering. In plants submitted to double stress, g_s was low (less than $0.15 \text{ mol m}^{-2} \text{ s}^{-1}$) and stable for a range of predawn leaf water potentials between -0.3 and -0.7 MPa .

Table 3. Parameter estimates of the non-rectangular hyperbola model of the photosynthetic irradiance response curve for the 4 treatments, control, water stress, fungal stress, and both stresses together. MAP_{max} , maximal net leaf photosynthetic rate of unstressed plant [$\mu\text{mol}(\text{CO}_2) \text{ m}^{-2} \text{ s}^{-1}$], MRUE_{max} , maximal radiation use efficiency of unstressed plant [$\text{mol}(\text{quantum}) \text{ mol}^{-1}(\text{CO}_2)$], m_{min} , minimal convexity index, SL_p [$\mu\text{mol}(\text{CO}_2) \text{ m}^{-2} \text{ s}^{-1} \text{ MPa}^{-1}$], SL_R [$\text{mol}(\text{quantum}) \text{ mol}^{-1}(\text{CO}_2) \text{ MPa}^{-1}$], and SL_m [MPa^{-1}], the slopes of the change of P_{Nmax} , MRUE , and m , respectively, against the predawn leaf water potential.

Parameter	Estimate	Asymptotic SE	Asymptotic 95 % confidence interval lower	upper
MAP_{max}	23.160	0.605	21.97	24.36
MRUE_{max}	0.0819	0.0046	0.0729	0.0909
m_{min}	0.410	0.023	0.361	0.458
SL_p	-2.00	0	-2.00	-2.00
SL_R	-1.223	0.039	-1.306	-1.153
SL_m	1.316	0.370	2.046	0.587

Discussion

In relation to the increase in number of brown rust lesions responsible for plant water losses, there was a Ψ_{wp} reduction in wheat leaves (Fig. 2B). On days 12 and 19, leaf rust and water stress had additive effects on Ψ_{wp} reduction: the reduction was -0.38 MPa in WS×FS treatment in comparison to -0.17 and -0.20 MPa in FS and WS treatments, respectively. Paul and Ayres (1984) made similar observations with groundsel infected by *Puccinia lagenophorae* and submitted to a post-infection drought. The combined effects of *P. lagenophorae* infection and drought led to a leaf water potential reduction of -1.74 MPa in comparison to healthy control plants, whereas FS and WS applied independently produced Ψ_{wp} reductions of -1.02 and -0.77 MPa , respectively.

The Ψ_{wp} response of the wheat plants depended on the number of infected leaves. With 5 infected leaves in comparison to only 3, there was a significant decrease in Ψ_{wp} corresponding to the larger diseased area on days 5, 12, and 19 after inoculation. When measuring leaf water potential during daytime hours, comparable results were obtained in barley infected by *Puccinia hordei* (Berryman *et al.* 1991) and in sugar beets infected by *Erysiphe polygoni* (Gordon and Duniway 1982).

To simulate the P_{N} -irradiance response under single or combined leaf rust and post-infection drought stresses, a model was built using a non-rectangular hyperbolic function of radiation with Ψ_{wp} -dependent parameters. After comparison with Li-6400 measurements, the P_{N} versus Ψ_{wp} model was tested using independent LCA3 ADC measurements obtained in the growth chamber under given irradiance ($500\text{--}600 \mu\text{mol m}^{-2} \text{ s}^{-1}$). With this

independent set of values, the relationship between measured P_{N} and Ψ_{wp} (Fig. 7A, *bold symbols*) was close to the modelled relationship based on Eq. 1 in Appendix (*open symbols*). The slopes of the linear regressions between measured or modelled P_{N} against Ψ_{wp} were 32.3 and 28.4, respectively, with corresponding r^2 coefficients of 0.87 and 0.99. Although these slope values are in the same range, they differ significantly at the 0.05 level. Compared to the P_{N} values measured in the growth chamber, the model output was rather satisfactory (regression slope = 0.76, $r^2 = 0.86$). The differences between model and measurements might be due to non-linearity of the three model parameters against Ψ_{wp} (Eqs. 2, 3, and 4 in Appendix). This confirmed the predominant role of Ψ_{wp} as a factor controlling P_{N} variation. At leaf scale, a unique relationship was found between P_{N} and Ψ_{wp} resulting from WS, FS, or WS×FS. The P_{N} reductions observed for each type of stress can be explained in one situation (WS) by a concomitant reduction in P_{N} and g_s (Fig. 4C), in another case (FS) by a reduction in P_{N} with no variation in g_s but with an increase in respiratory processes indicated by a doubling of Γ together with a decrease in mesophyll conductance that indicates a decrease in carboxylation efficiency (Fig. 4B).

There is a controversy over the mechanisms by which stress decreases P_{N} and the regulation between these mechanisms (Cornic 2000). Three principal mechanisms are invoked: (1) restricted diffusion of CO_2 caused by stomata closure (Bethenod *et al.* 1996), (2) inhibition of CO_2 metabolism caused by the reduction of ribulose-1,5-bisphosphate synthesis whose intensity is shown by

mesophyll conductance, and (3) change in the ratio between oxygenase and carboxylase activities of ribulose-1,5-bisphosphate carboxylase/oxygenase (RuBPCO) shown by variation in Γ (Cornic 1994).

The P_N decrease could not be explained by stomata closure in infected plants (Fig. 4B). Ψ_{wp} decrease revealed a dehydration in infected plants (Fig. 2). In both FS and WS×FS treatments, the observed increase of Γ (Fig. 4B,D) indicated the occurrence of the third mechanism with the increase of oxygenase activity of RuBPCO in response to dehydration. In all treatments, the decrease of mesophyll conductance (initial slope of the P_N-C_i response curve) was linked to Ψ_{wp} decrease, therefore no conclusion could be made concerning the role of the second mechanism to discriminate between stress effects (Fig. 4).

In the present study, the analysis of plant development over time indicated differences in leaf growth. This is consistent with the cell growth sensitivity to plant water stress (Hsiao 1973). FS caused by *P. recondita* and WS had additive deleterious effects on the development of leaves 5 (infected) and 7 (non-infected, Table 2) as well as on plant dry matter production. However, for whatever leaf number (5, 7, top leaf), the reduction in leaf area of FS treatment was almost constant (15 %). In the WS treatment the leaf area was reduced by 19 (leaf 5) to 51 (non-infected top leaf) %. In the WS and FS treatments, Ψ_{wp} were similar. These results along with the differences in leaf area reduction in response to each type of stress suggest the existence of an effect compensating the water stress impact on non-inoculated leaves. Leaf expansion is one of the first processes affected by WS, therefore the growth of new leaves in the WS treatment was more strongly affected than the growth of leaves which appeared before the stress occurred. In the WS×FS treatment, the area reduction of non-infected top leaves corresponded approximately to the average of both area reductions observed on WS and FS treatments applied independently, and not to their sum as in the case of leaves 5 and 7. This observation is consistent with the existence of a compensatory effect that can be assessed by the difference of leaf area reduction (expressed as % of control treatment) between the single WS and FS treatments. Benefiting to the FS treatment, this compensatory effect was low (4.0 %) on leaf 5, intermediate (18.5 %) on leaf 7, and high (34.5 %) on top leaf, respec-

tively. Such effect could explain the lower reduction in the area of top leaves in the WS×FS treatment (34 %) compared to the WS treatment (51 %). Thus, the infected plant is partially able to resist rust infection in upper, uninfected leaves of wheat similarly as shown by Murray and Walters (1992) for rusted broad bean.

Stomata behaviour is very different between inoculated (FS and WS×FS treatments) and non-inoculated plants (control and WS treatments). In non-inoculated plants, the $g_s\text{CO}_2$ decrease with predawn water potential (Ψ_{wp} , Fig. 7B) together with P_N decrease (Fig. 7A) induce a C_i constancy close to 200 $\mu\text{mol mol}^{-1}$ (Fig. 4C). In inoculated plants, stomata behaviour was more erratic: after sporulation, the transient increase of g_s in FS treatment or the g_s stability in WS×FS treatment close to 0.15 $\text{mol m}^{-2} \text{s}^{-1}$, lead to a C_i increase, when P_N decreased (Fig. 4B,D). In the FS treatment the transient increase of g_s stopped after 3 d and the difference in g_s values disappeared between irrigated treatments (control and FS) as between water stressed treatments (WS and WS×FS) even though Ψ_{wp} values were different (Fig. 7B). This is not consistent with previous works dealing with stomata closure in response to chemical messages. Such is the case for *Septoria nodorum* in wheat (Bethenod *et al.* 1982) and *Helminthosporium maydis* in corn (Arntzen *et al.* 1973). In the case of brown rust, no specific chemical message has been discovered. Therefore the mechanical changes in diseased leaves are likely to generate a water status modification.

In conclusion, Ψ_{wp} is a pertinent indicator of plant response to a single stress (brown rust infection or soil water deficit) or a twofold stress in the chosen experimental conditions. If both brown rust infection and post-infection drought produce similar changes in Ψ_{wp} , these stresses lead to a similar physiological strain (reduction in P_N by means of different mechanisms of gas exchange regulation) and a similar damage (reduction in plant growth).

It is helpful to invoke the concept of stress response interaction outlined by Higley *et al.* (1993). In the case of dry matter of infected plants, area of infected leaves, and photosynthesis, the effects of fungal infection and post-infection drought on P_N were additive, and no stress interaction was found. In the case of g_s and leaf area of non-infected top leaves, there was an interaction between the responses to fungal infection and post-infection drought.

References

Arntzen, C.J., Haugh, M.F., Bobick, S.: Induction of stomatal closure by *Helminthosporium maydis* pathotoxin. — *Plant Physiol.* **52**: 569-574, 1973.

Ayres, P.G.: Effect of disease on plant water relations. — In: Ayres, P.G. (ed.): *Effects of Disease on the Physiology of the Growing Plant*. Pp. 131-148. Cambridge University Press, Cambridge 1981.

Balasubramanian, R., Gaunt, R.E.: The effects of fungicide sprays on root development, yield and yield components of wheat in the absence of disease. — *Plant Protect. Quart.* **4**: 95-97, 1990.

Berghaus, R., Reisener, H.J.: Changes in photosynthesis of wheat plants infected with wheat stem rust (*Puccinia graminis* f.sp. *tritici*). — *Phytopathol. Z.* **112**: 165-172, 1985.

Berryman, C.A., Eamus, D., Farrar, J.F.: Water relations of leaves of barley infected with brown rust. – *Physiol. mol. Plant Pathol.* **38**: 393-405, 1991.

Bethenod, O., Bousquet, J.F., Laffray, D., Louguet, P.: Réexamen des modalités d'action de l'ochracine sur la conductance stomatique des feuilles de plantules de blé, *Triticum aestivum* L., cv "Etoile de Choisy". – *Agronomie* **2**: 159-166, 1982.

Bethenod, O., Tardieu, F., Katerji, N.: Relationship between net photosynthetic rate and stomatal conductance in leaves of field-grown maize subjected to soil compaction or soil drying. – *Photosynthetica* **32**: 367-379, 1996.

Caemmerer, S. von, Farquhar, G.D.: Some relationships between the biochemistry of photosynthesis and the gas exchange of leaves. – *Planta* **153**: 376-387, 1981.

Cannell, M.G.R., Thornley, J.H.M.: Temperature and CO₂ responses of leaf and canopy photosynthesis: A clarification using the non-rectangular hyperbola model of photosynthesis. – *Ann. Bot.* **82**: 883-892, 1998.

Cornic, G.: Drought stress and high light effects on leaf photosynthesis. – In: Baker, N.R., Bowyer, J.R. (ed.): *Photoinhibition of Photosynthesis from Molecular Mechanisms to the Field*. Pp. 297-313. BIOS Scientific Publ., Oxford 1994.

Cornic, G.: Drought stress inhibits photosynthesis by decreasing stomatal aperture – not by affecting ATP synthesis. – *Trends Plant Sci.* **5**: 187-188, 2000.

Cowan, M.C., Van der Wal, A.F.: An ecophysiological approach to crop losses: exemplified in the system of wheat leaf rust and glume blotch. IV: Water flow and leaf water potential of uninfected wheat plants and plants infected with *Puccinia recondita* f. sp. *triticina*. – *Neth. J. Plant Pathol.* **81**: 49-57, 1975.

Duniway, J.M., Durbin, R.D.: Some effects of *Uromyces phaseoli* on the transpiration rate and stomatal response of bean leaves. – *Phytopathology* **61**: 114-119, 1971.

Geagea, L., Huber, L., Sache, I.: Dry-dispersal and rain-splash of brown (*Puccinia recondita* f. sp. *tritici*) and yellow (*P. striiformis*) rust spores from infected wheat leaves exposed to simulated raindrops. – *Plant Pathol.* **48**: 472-482, 1999.

Gordon, T.R., Duniway, J.M.: Stomatal behavior and water relations in sugar beet leaves infected by *Erysiphe polygoni*. – *Phytopathology* **72**: 723-726, 1982.

Higley, L.G., Browde, J.A., Higley, P.M.: Moving towards new understandings of biotic stress and stress interactions. – In: Buxton, D.R. et al. (ed.): *International Crop Science*. Vol. I. Pp. 749-754. CSSA, Madison 1993.

Hsiao, T.C.: Plant responses to water stress. – *Annu. Rev. Plant Physiol.* **24**: 519-570, 1973.

Johnson, D.A., Richards, R.A., Turner, N.C.: Yield, water relations, gas exchange, and surface reflectances of near-isogenic wheat lines differing in glaucousness. – *Crop Sci.* **23**: 318-325, 1983.

McGrath, M.T., Pennypacker, S.P.: Alteration of physiological processes in wheat flag leaves caused by stem rust and leaf rust. – *Phytopathology* **80**: 677-686, 1990.

Murray, D.C., Walters, D.R.: Increased photosynthesis and resistance to rust infection in upper, uninjected leaves of rusted broad bean (*Vicia faba* L.). – *New Phytol.* **120**: 235-242, 1992.

Okwulehie, I.C.: Translocation of ¹⁴C-(labelled) photosynthates in groundnut (*Arachis hypogaea* L.) infected with *Macrophomina phaseoli* (Maub) Ashby. – *Photosynthetica* **38**: 473-476, 2000.

Paul, N.D., Ayres, P.G.: Effects of rust and post-infection drought on photosynthesis, growth and water relations in groundsel. – *Plant Pathol.* **33**: 561-569, 1984.

Prioul, J.L., Chartier, P.: Partitioning of transfer and carboxylation components of intracellular resistance to photosynthetic CO₂ fixation: A critical analysis of the methods used. – *Ann. Bot.* **41**: 789-800, 1977.

SAS Institute: *SAS/STAT User's Guide, Version 6.03*. – SAS Institute, Cary 1988.

Shtienberg, D.: Effect of foliar diseases of wheat on the physiological processes affecting yield under semi-arid conditions. – *Plant Pathol.* **40**: 533-541, 1990.

Shtienberg, D.: Effects of foliar diseases on gas exchange processes: A comparative study. – *Phytopathology* **82**: 760-765, 1992.

Spotts, R.A., Ferree, D.C.: Photosynthesis, transpiration, and water potential of apple leaves infected by *Venturia inaequalis*. – *Phytopathology* **69**: 717-719, 1979.

Statler, G.D.: Apparent photosynthesis in healthy and *Puccinia recondita* infected wheat plants. – *Can. J. Plant Pathol.* **10**: 203-206, 1988.

Tardieu, F., Katerji, N.: Plant response to the soil water reserve: Consequences of the root system environment. – *Irrig. Sci.* **12**: 145-152, 1991.

Tissera, P., Ayres, P.G.: Transpiration and the water relations of faba bean (*Vicia faba*) infected by rust (*Uromyces viciae-fabae*). – *New Phytol.* **102**: 385-395, 1986.

Turner, N.C., Graniti, A.: Fusicoccin: A fungal toxin that opens stomata. – *Nature* **223**: 1070-1071, 1969.

APPENDIX

Determination of the parameters of non-rectangular hyperbola model of photosynthetic irradiance response curve

The dependence of leaf net photosynthetic rate (P_N , $\mu\text{mol m}^{-2} \text{s}^{-1}$) on irradiance [photosynthetic photon flux density, PPFD; $\mu\text{mol(quantum)} \text{m}^{-2} \text{s}^{-1}$] is described by a non-

rectangular hyperbola (Prioul and Chartier 1977, Cannell and Thornley 1998):

$$P_N = R_D + \{ \text{MRUE PPFD} + P_{N\max} - [(\text{MRUE PPFD} + P_{N\max})^2 - 4 \text{ m MRUE PPFD} P_{N\max}]^{0.5} \} / 2 \text{ m} \quad (1)$$

where MRUE is the quantum yield of CO₂ assimilation based on irradiance that represents the initial slope of the hyperbola, $P_{N\max}$ is the irradiance-saturated photosyn-

thesis, m the convexity index of the hyperbola (dimensionless), and R_D the dark respiration rate.

Because R_D is a result of processes other than photo-

synthesis, our first assumption was that R_D was constant with a mean value of $1.6 \mu\text{mol m}^{-2} \text{s}^{-1}$. In order to test the dependence of the irradiance- P_N relationship to the internal water status, we used the response of the three parameters, MRUE, $P_{N\max}$, and m , to the predawn leaf water potential (Ψ_{wp}) in wheat (Johnson *et al.* 1983, Tardieu and Katerji 1991). To achieve this, we determined the maximal value of MRUE and $P_{N\max}$, MRUE_{max}, and MAP_{max}, respectively, and the minimal value of m (m_{\min}) based on existing knowledge (Hsiao 1973) for $\Psi_{wp} = 0.2 \text{ MPa}$.

We assumed that MRUE and $P_{N\max}$ are linearly de-

creasing and m is linearly increasing as Ψ_{wp} decreases. Let SL_R , SL_P , and SL_m be the slope of the linear response of MRUE, $P_{N\max}$, and m , respectively.

$$\text{MRUE} = \text{MRUE}_{\max} [1 - SL_R (\Psi_{wp} + 0.2)] \quad (2)$$

$$P_{N\max} = \text{MAP}_{\max} [1 - SL_P (\Psi_{wp} + 0.2)] \quad (3)$$

$$m = m_{\min} [1 - SL_m (\Psi_{wp} + 0.2)] \quad (4)$$

We substituted MRUE, $P_{N\max}$, and m relations in Eq. (1). Then the NLIN procedure of the Statistical Analysis System (SAS 1988) was used with the Marquardt method to determine the parameters in Eqs. 2, 3, and 4.